



Providing Choice & Value
Generic CT and MRI Contrast Agents



CONTACT REP

AJNR

Imaging the Internal Auditory Canal with an 8 × 2 Transceiver Array Head Coil at 7T

A. Nada, J.P. Cousins, A. Rivera, S.B. Carr, J. Jones, C. Minor, H.P. Hetherington, J.H. Kim and J.W. Pan

AJNR Am J Neuroradiol published online 27 March 2025
<http://www.ajnr.org/content/early/2025/03/27/ajnr.A8569>

This information is current as
of July 29, 2025.

Imaging the Internal Auditory Canal with an 8 × 2 Transceiver Array Head Coil at 7T

A. Nada, J.P. Cousins, A. Rivera, S.B. Carr, J. Jones, C. Minor, H.P. Hetherington, J.H. Kim, and J.W. Pan



ABSTRACT

SUMMARY: 7T neuroimaging has known problems with B_1^+ strength, homogeneity and B_0 susceptibility that make imaging in the inferior brain regions difficult. We investigated the utility of a decoupled 8 × 2 transceiver coil and shim insert to image the internal auditory canal (IAC) and inferior brain in comparison to the standard Nova 8/32 coil. B_1^+ , B_0 , and the T2 sampling perfection with application-optimized contrasts by using flip angle evolution sequence (SPACE) were compared by using research and standard methods in $n = 8$ healthy adults by using a Terra system. A T2 TSE was also acquired, and 2 neuroradiologists evaluated structures in and around the IAC, blinded to the acquisition, by using a 5-point Likert scale. The Nova 8/32 coil gave lower B_1^+ inferiorly compared with the whole brain while the transceiver maintained similar B_1^+ throughout. SPACE images showed that the transceiver performed significantly better, e.g., the transceiver scored 4.0 ± 0.8 in the left IAC, compared with 2.5 ± 0.8 with the Nova 8/32. With T2-weighted imaging that places a premium on refocusing pulses, these results show that with improved B_1^+ performance inferiorly, good visualization of the structure of the IAC and inferior brain regions is possible at 7T.

ABBREVIATIONS: IAC = internal auditory canal; pTx = parallel transmit; RF = radiofrequency; SAR = specific absorption rate; SPACE = sampling perfection with application-optimized contrasts by using flip angle evolution; VHOS = very high order B_0 shim

With its higher SNR, increased spectral dispersion, and increasing clinical availability, 7T MRI has demonstrated capability to more frequently identify subtle lesions for patients with epilepsy and multiple sclerosis than at 3T.¹⁻³ However, for pathologies occurring in the posterior fossa, obtaining sufficient image quality is known to be challenging. With single transmit coil designs, the shortened electromagnetic wavelength⁴ at ultra-high field has been linked with loss of contrast and/or signal loss in the lateral temporal lobes and cerebellum, depending on the applied pulse sequence. For example, spin-echo images commonly show B_1^+ based shading problems while SWI does not. B_0 inhomogeneity is also a well-known independent problem, with strong

susceptibility gradients from anatomic interfaces (eg, air-bone-brain⁵) at the skull base. In these regions, the B_1^+ and B_0 effects can combine to further degrade image quality, particularly for pulse sequences with limited radiofrequency (RF) bandwidth.

Multiple transmit coils provide better performance, with most ultra-high-field systems now available with 8-channel transmit capability. However, T2-weighted image quality with the commonly used parallel transmit (pTx) coil (Nova 8/32) is suboptimal inferiorly.^{6,7} The 8 × 2 inductively decoupled transceiver provides an alternative coil that can improve image quality in the inferior brain.⁷ The transceiver gives improved B_1^+ homogeneity by its increased number (16 channels) of transmit elements and limiting interelement interactions through its decoupled design. This performance can be augmented by a B_0 shim insert,^{8,9} which improves whole brain B_0 homogeneity by approximately 50% in comparison to vendor shimming. This report compares the image quality in the internal auditory canal (IAC) and inferior brain region between the standard (Nova 8/32, vendor shimming) and research (transceiver, shim insert) strategies as assessed by 2 neuroradiologists, blinded to the type of acquisition.

Received June 26, 2024; accepted after revision October 7.

From the Washington University in St. Louis (A.N.), School of Medicine, Mallinckrodt Institute of Radiology, St. Louis, Missouri; Departments of Radiology (J.P.C., J.J., C.M., J.H.K., J.W.P.), Otolaryngology (A.R.), and Neurosurgery (S.B.C.), University of Missouri, Columbia, Missouri; and Resonance Research Inc. (H.P.H.), Billerica, Massachusetts.

This research has been supported by the U.S. Department of Health and Human Services, National Institutes of Health, Office of Strategic Coordination, Common Fund, NIH NIBIB EBO24408.

Please address correspondence to Ayman Nada, MD, Washington University in St. Louis, School of Medicine, Mallinckrodt Institute of Radiology, St. Louis, MO, 63110; e-mail: anada@wustl.edu; @amn_med09; @Mizzou



Indicates article with supplemental data.



This article contains an [imaging protocol](#) available on our website.

<http://dx.doi.org/10.3174/ajnr.A8569>

MATERIALS AND METHODS

This prospective study was conducted with University of Missouri institutional review board approval and followed the Strengthening the Reporting of Observational studies in Epidemiology guidelines

Table 1: Ratings for T2 SPACE, comparing Nova 8/32 and transceiver coils

	Left IAC	Right IAC	Left Trigem	Right Trigem	CBL	Temporal	Brainstem
T2 SPACE							
Nova 8/32	2.5 ± 0.8	1.4 ± 0.9	3.7 ± 0.9	3.7 ± 0.9	3.1 ± 1.2	2.5 ± 0.8	3.2 ± 1.1
8 × 2 transceiver	4.0 ± 0.8	3.8 ± 1.0	4.4 ± 0.6	4.4 ± 0.6	4.1 ± 0.6	3.4 ± 0.7	3.9 ± 0.9
Ratio	1.76 ± 0.72	1.65 ± 0.74	1.23 ± 0.30	1.25 ± 0.30	1.47 ± 0.48	1.44 ± 0.45	1.30 ± 0.33
Two-tailed unpaired <i>P</i> values	< .001	< .001	< .05	< .05	< .005	< .005	< .05

Note:—CBL indicates cerebellum; IAC, internal auditory canal; SPACE, sampling perfection with application-optimized contrasts by using flip angle evolution; Trigem, Trigeminal.

Table 2: Ratings for T2 3D TSE, all acquired with transceiver

T2 3D TSE	IAC	Trigem <i>n</i>	VC <i>n</i>	Facial <i>n</i>	Cochlea <i>n</i>	Nervus Intermed	Superior Vestib <i>n</i>	Inferior Vestib <i>n</i>
Left	4.6 ± 0.4	4.6 ± 0.5	4.6 ± 0.4	4.7 ± 0.5	4.5 ± 0.7	2.6 ± 0.6	4.0 ± 0.9	3.6 ± 0.9
Right	4.6 ± 0.5	4.6 ± 0.5	4.4 ± 0.7	4.4 ± 0.5	4.3 ± 0.8	2.8 ± 0.8	3.9 ± 0.5	3.5 ± 0.7
	Falciform crest+Bells	Cochlea (interscalar sep, modiolus)		Basal scala media	Superior semicirc canal (ant limb)	Lateral semicirc canal	Posterior semicirc canal	
Left	2.6 ± 0.6	4.3 ± 0.6		2.2 ± 1.3	4.3 ± 0.7	3.5 ± 1.2	3.9 ± 1.2	
Right	2.5 ± 0.5	4.1 ± 0.6		2.0 ± 1.4	4.4 ± 0.7	3.7 ± 1.4	4.4 ± 0.8	

For all ratings, the 5-point Likert scale is used: 1, not visible; 2, visible but with complete loss of detail; 3, visualization of some anatomic detail; 4, visualization of most anatomic detail; 5, perfect visualization of anatomic detail.

Note:—IAC indicates internal auditory canal; VC, Vestibulocochlear; Trigem, Trigeminal; Intermed, Intermedius; Vestib, Vestibular; *n*, Nerve.

(Supplemental Data). T2 sequences (particularly the sampling perfection with application-optimized contrasts by using flip angle evolution [SPACE; Siemens] sequence) were established given their dominant role in IAC imaging. Comparison images were acquired in $n = 8$ healthy adults (mean age 35.3 ± 18.0 , range 21–63), evaluating vendor (by using the Nova 8/32, Nova Medical, RF B_1^+ shimming and standard B_0 shimming) and research methods (by using the 8×2 decoupled transceiver, Resonance Research; RF B_1^+ shimming and research B_0 shimming^{8,10}). The transceiver has available safety monitoring data (virtual observation point files), however, has not gone through FDA review. With high contrast seen from TSE images,¹¹ we also acquired T2-weighted 3D TSE images and T1 FLAIR 2D TSE images as the basic elements of the IAC protocol.

RF Coil Strategies

A 7T pTx Terra system (Siemens) with 8 pTx channels was used throughout. With the SPACE acquisition, each volunteer was imaged by using the 2 different RF coils and B_0 shimming methods. For each strategy, the parameters were optimized by using the available individual methods.

The Nova 8/32 coil used the RF and B_0 shimming with vendor supplied hardware and software. Minimal differences were observed in image quality when RF shim settings of patient versus volume specific over the target region were used (Supplemental Data). To provide a more consistent B_1^+ profile for whole-brain imaging that typically targets an RF amplitude of $11.7 \mu\text{T}$ (500 Hz), patient-specific RF shimming was used. For B_0 shimming, first, second, and 4 third-order shims (Terra standard) were used.

For the research strategy, the transceiver was tuned and matched for each volunteer (required <1.5 minutes). RF shimming (phase and amplitude) was performed as described¹⁰ targeting $11.7 \mu\text{T}$ amplitude over the intracranial volume (ie, equivalent to patient-specific RF shimming). Because of a lack of clear superiority for regional (IACs and surrounding structures) versus whole-brain RF shimming, a whole-brain optimization was used (equivalent to the vendor patient-specific optimization). For B_0 shimming,

the transceiver's compact size enables use within a very high order B_0 shim (VHOS) insert, providing 7 third-order shims and 8 fourth-order shims.⁸ We were unable to do this with the Nova 8/32 because it did not fit within the VHOS.

For both coils, vendor-determined reference voltages were used.

Imaging Sequences

T2 SPACE¹² images were evaluated by 2 board certified neuro-radiologists, blinded to the acquisition. These images were acquired at 0.6 mm^3 resolution, TR/TE of 2.8 s/140 ms covering a $160 \times 160 \times 50 \text{ mm}$ FOV, acquisition time 7:02. For this group, $n = 9$ (5 women, 4 men) subjects were recruited; 1 male subject was unable to completely fit within the transceiver, leaving $n = 8$ subjects.

For the T2 TSE, we previously showed that the transceiver is superior in SNR in the inferior brain region to the Nova 8/32,⁷ thus to avoid duplicative work, the TSE was acquired only in the research strategy. A total of $n = 8$ subjects were studied at 0.6 mm^3 resolution, TR/TE of 3 s/169 ms covering $172 \times 172 \times 25 \text{ mm}$ FOV, acquisition time 7:15. To define a reasonable clinical protocol, we also acquired T1-weighted FLAIR 2D TSE images. The T1-weighted images were not evaluated for image quality, because the role of the T1-weighting is to provide contrast with gadolinium, which was not available for this study. For demonstration purposes with the T2 TSE, $n = 3$ subjects were each studied with vendor and research methods. For all studies, first level specific absorption rate (SAR) monitoring was used, with values typically ranging between 85%–99%.

Radiologic Evaluation

Tables 1 and 2 show the anatomic structures evaluated with the SPACE and TSE data and the 5-point Likert scale. The comparison between the 2 strategies was tested for significance by using unpaired 2-tailed *t* tests. To demonstrate the sensitivity to IAC pathology, images from $n = 3$ patients with known vestibular schwannomas are shown in the Supplemental Data. The imaging parameters are also shown in the Supplemental Data.

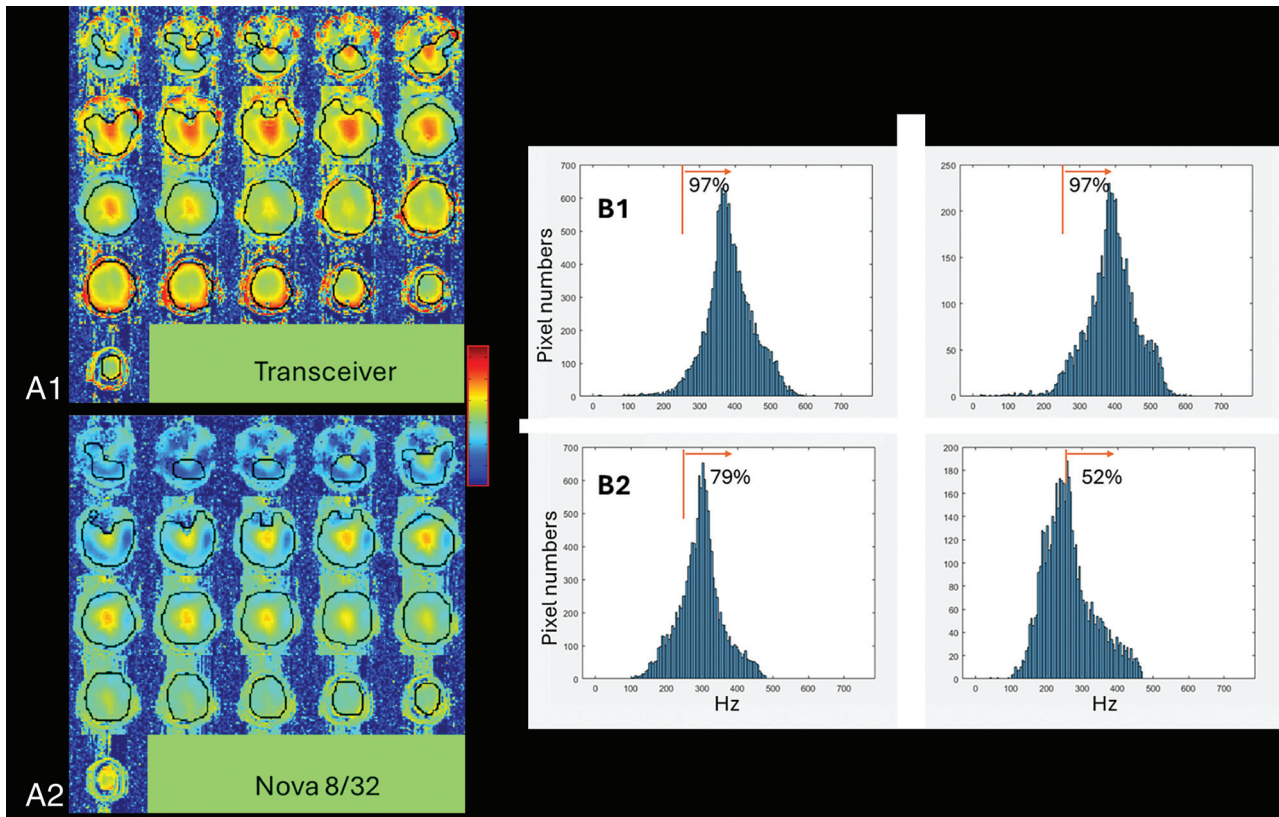


FIG 1. Comparison of B_1^+ from the 2 RF coils, (A) shows the simultaneous transmission B_1^+ maps and (B) shows histogram distributions. (A1, B1) are from the transceiver; (A2, B2) from the Nova 8/32 coil. In (A), the B_1^+ maps are scaled identically and show the ROIs (black outlines). In B, histograms of B_1^+ values, from either the whole brain (left) or the inferior brain (right). For the whole brain, all slices are included; for the inferior brain, pixels from the 9 most inferior slices were used. The orange line identifies the 250 Hz threshold with the indicated percentages (F_{250} , fraction of pixels above 250 Hz). For A and B, patient specific RF shimming was performed over the whole head with Siemens standard reference voltages applied to generate the measured B_1^+ . All data are shown from a single volunteer.

RESULTS

B_1^+ and B_0 Comparison

Figure 1A shows the B_1^+ maps from a volunteer acquired with the transceiver and Nova 8/32. For the transceiver, over the group of $n = 8$ subjects, whole-brain RF shimming achieved a mean whole-brain B_1^+ $9.1 \pm 0.4 \mu\text{T}$ (mean, SD across subjects). In the IAC itself there is little signal available to measure B_1^+ performance; however, the mean B_1^+ achieved across the group over the surrounding tissue in the inferior brain region (see Fig 1 for volumes) was $9.2 \pm 0.3 \mu\text{T}$, yielding a within-subject ratio of achieved B_1^+ whole brain/inferior brain of 0.98 ± 0.02 . To characterize the variation in B_1^+ over the ROIs, we determined the fraction of pixels, F_{250} , with B_1^+ greater than 250 Hz, ie, $>5.8 \mu\text{T}$ (this is 50% of the typically targeted B_1^+ of $11.7 \mu\text{T}$). F_{250} was determined with each ROI; for the subject shown in Fig 1, the number of pixels is approximately 14,000 for the whole brain; approximately 5000 for the inferior brain. For the transceiver, the F_{250} was $96.0\% \pm 1.1\%$ for whole brain versus $95.4\% \pm 1.7\%$ inferiorly (Fig 1B).

For the Nova 8/32 acquired with patient-specific RF shimming, the group averages and standard deviation for the B_1^+ means in the whole brain and inferior brain regions were $6.7 \pm 0.1 \mu\text{T}$ and $6.2 \pm 0.2 \mu\text{T}$, respectively. The lower B_1^+ obtained with the Nova 8/32 is due vendor-based reference voltage optimization. The F_{250} was substantially smaller than the transceiver, achieving $76.6\% \pm 4.0\%$ and $49.4\% \pm 7.2\%$ over the whole brain and inferior brain regions,

respectively. The histograms for F_{250} (Fig 1B) show a skewed B_1^+ distribution from the Nova 8/32 inferiorly while the distributions are similar between inferior and whole brain for the transceiver.

Figure 2 shows the whole brain B_0 maps after shimming, comparing the vendor and research methods. From $n = 8$ subjects with the vendor shimming, the mean intracranial whole-brain SD σ_{WB,B_0} was 47 ± 9 Hz, which was substantially worse than the 30 ± 7 Hz achieved when using the research shimming routines. Inclusion of VHOS hardware further reduced the achieved σ_{WB,B_0} to 24 ± 5 Hz.

T2 SPACE and TSE Images with Radiologic Evaluation

Figure 3A shows the T2 SPACE images comparing the transceiver and Nova 8/32. Although the Nova coil typically demonstrates excellent signal retention through the central brainstem region, there is a substantial shading in signal intensity laterally into the auditory canals, temporal lobes, and cerebellar hemispheres. In contrast, the transceiver exhibited superior signal retention laterally. Figure 3B shows matched T2 TSE images. The performance appears more comparable between the 2 coils but is consistent with previous data⁷ showing the high SNR with transceiver giving greater clarity for identification of the nerve roots.

Table 1 summarizes the radiologic image quality evaluation for the SPACE images comparing the 2 coil strategies. Two-tailed unpaired t tests showed significantly better visibility for all structures

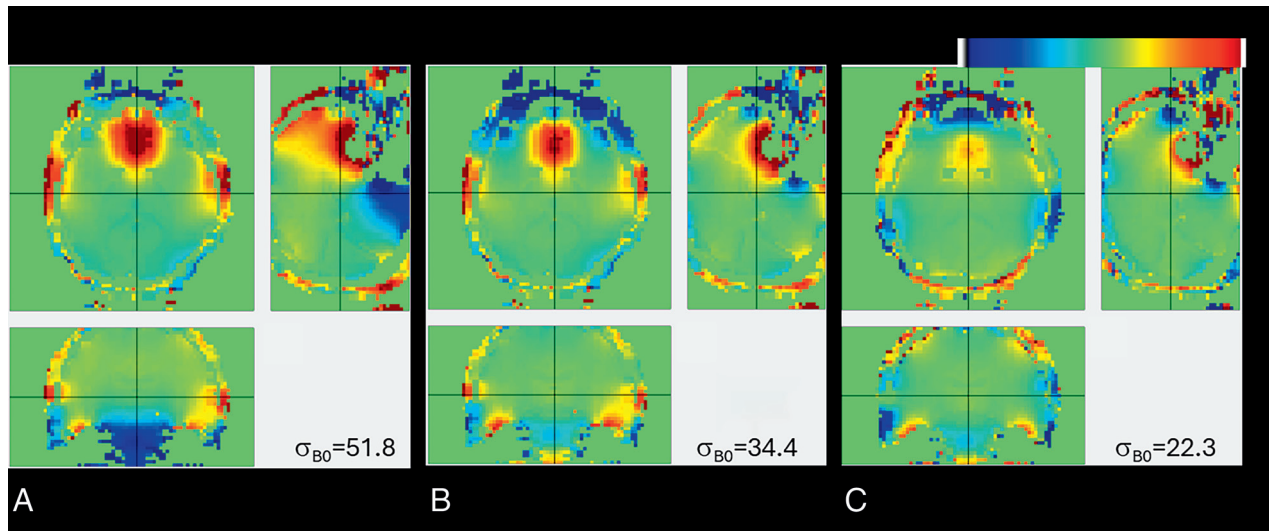


FIG 2. B_0 maps acquired after shimming from a matched subject, (A) standard shimming; (B) research software shimming methods and vendor shim hardware; and (C) research shim software and hardware (VHOS). For this subject, the mean σ_{B_0} (Hz) over the intracranial regions were 51.8, 34.4, and 22.3, respectively. σ_{B_0} = standard deviation of B_0 field.

considered with the transceiver; P values ranged from $< .001$ to $.05$. Table 2 summarizes the radiologic image quality for the TSE images from the transceiver. The transceiver's ability to detect pathology in patients with schwannoma is shown in the Supplemental Data with a listing of the imaging parameters.

DISCUSSION

B_1 and B_0 Performance

At 7T, the middle and posterior fossae are commonly difficult to image due to low amplitude and inhomogeneous B_1^+ as well as extensive B_0 inhomogeneity. In the Nova 8/32, Fig 1 (histograms) shows that inferiorly, the B_1^+ is down-shifted compared with the whole brain. In comparison, the transceiver maintains similar B_1^+ performance whether targeting inferior or whole brain regions. Consistent with this and previous work,^{7,10} the SPACE data (Fig 3) with the transceiver demonstrates improved image contrast compared with the Nova 8/32 inferiorly. The source of this inferior B_1^+ improvement is due to the 2 rows with increased number of transmit loop elements^{13,14} (8 each row) and their decoupled design,¹⁵ which enables better control over the transmission B_1^+ (the 16 elements of the 8×2 transceiver are powered in the 8-channel Terra by using 8 splitters). The B_1^+ performance can likely be further improved by providing more flexible control per transmission element, eg, a 16-channel transmit system driving each element independently. Furthermore, this study was performed by using solely RF shimming (ie, the same RF waveform to each RF channel); more optimal performance might be further achieved through use of full parallel RF transmission.^{15,16}

Due to the small size of the IACs and other nerves, it is difficult to obtain an accurate measurement of the B_0 values across them. In these data, with standard workflow we did not see a significant change in IAC image quality with the research strategies for shimming, although it clearly affected the image quality of the inferior frontal lobe as shown in the SPACE images (Fig 4).

Image Quality Between the Two Strategies

With the number of different hardware and software methods implemented, it is useful to consider which components exhibit the greatest effect for image quality. At 7T, the choice of sequence has impact on image quality because of the sequence's sensitivity to B_1^+ and B_0 performance (eg, the SPACE sequence has sensitivity to both¹²), which will vary depending on target anatomy. Thus, Figs 1 and 2 show the B_1^+ and B_0 performances; Fig 3 shows their integrated impact. For B_1^+ , the transceiver was able to maintain a relatively consistent B_1^+ distribution throughout the whole and inferior brain regions. In comparison, the Nova 8/32 exhibited a downward shift of the B_1^+ amplitudes inferiorly, causing this coil's limited z-coverage.

The impact of B_0 on image quality is known to be a function of B_1^+ and target anatomy (ie, susceptibility). With insufficient B_1^+ amplitude, the bandwidth of the slab or slice selection is limited, which when combined with poor B_0 inhomogeneity, will result in signal loss. Although without a detailed knowledge of the SPACE pulse sequence, it is difficult to quantify the impact of poor B_0 shimming, we can empirically consider this question. Figure 4A shows that with the transceiver operating at normal B_1^+ , the SPACE sequence generates reasonable signal intensity at the level of the temporal lobe and IAC-cerebellum. There is some signal loss over the inferior frontal lobe which improves with research B_0 shimming, while at the IAC-cerebellum level, the images appear appropriate with minimal sensitivity to research shimming. To examine the interaction between B_1^+ and B_0 , Fig 4B shows the matched images but acquired with 33% lower B_1^+ . As expected under low B_1^+ , there is an overall decrease in SNR compared with the normal B_1^+ acquisition. However, the standard shimmed images now show shading artifacts through the cerebellum and temporal lobe, while the matched research shimmed images in the IAC-cerebellum region show improved image consistency (a similar but smaller effect is seen in the temporal lobe). This is consistent with the limited bandwidth of the SPACE sequence: if the B_1^+ is adequate, requirement for

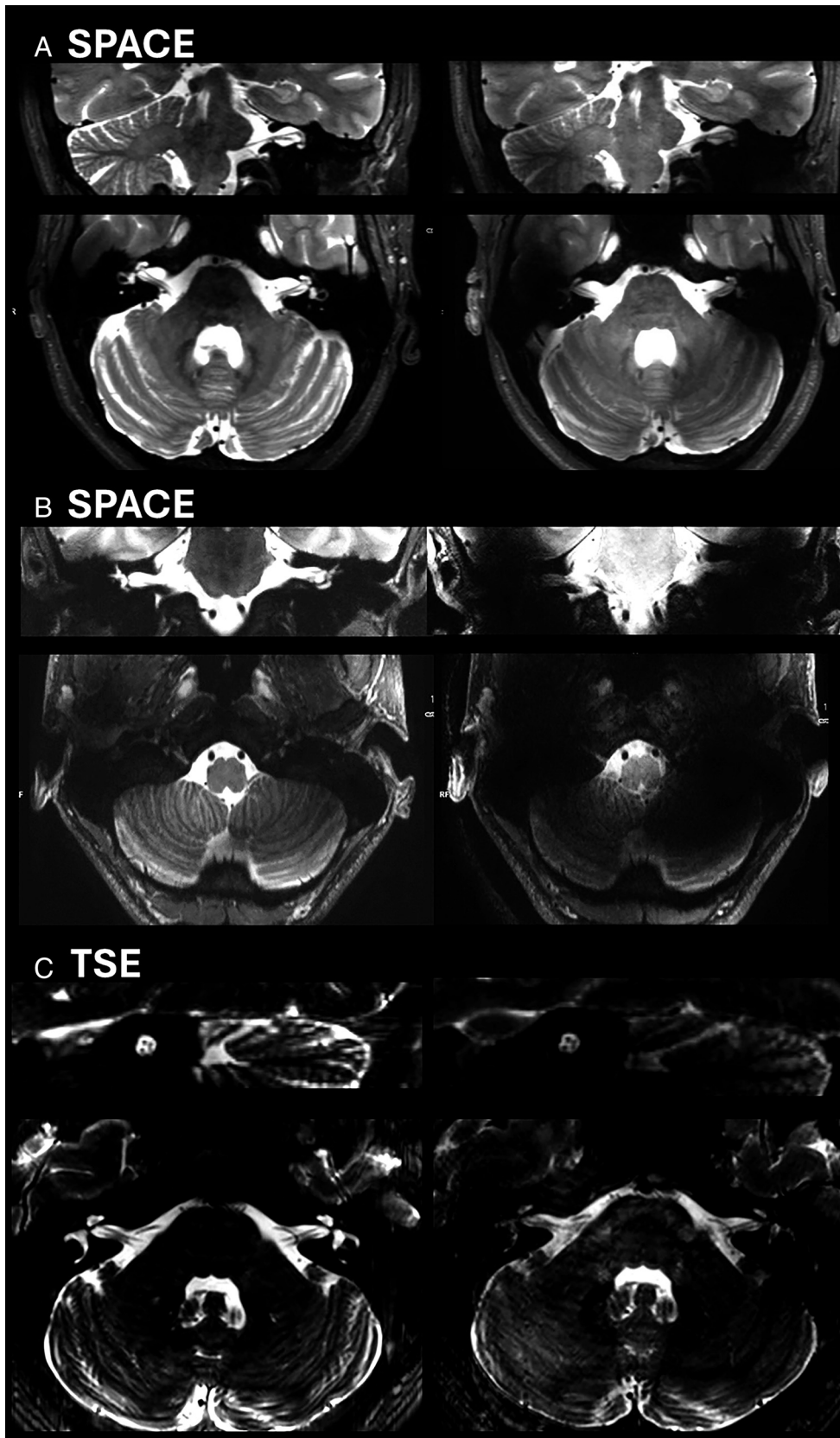


FIG 3. T2-weighted images. *A*, T2 SPACE axial and coronal images are shown from the level of the IAC. *B*, T2 SPACE axial and coronal images are shown from the level of the rostral medulla. *C*, T2 TSE axial and sagittal images targeting the IAC. The images on the left were acquired with the transceiver RF coil and the VHOS. The images on the right were acquired with the Nova 8/32. All panels are scaled identically between the transceiver and Nova 8/32. No additional image filtering or denoising was applied.

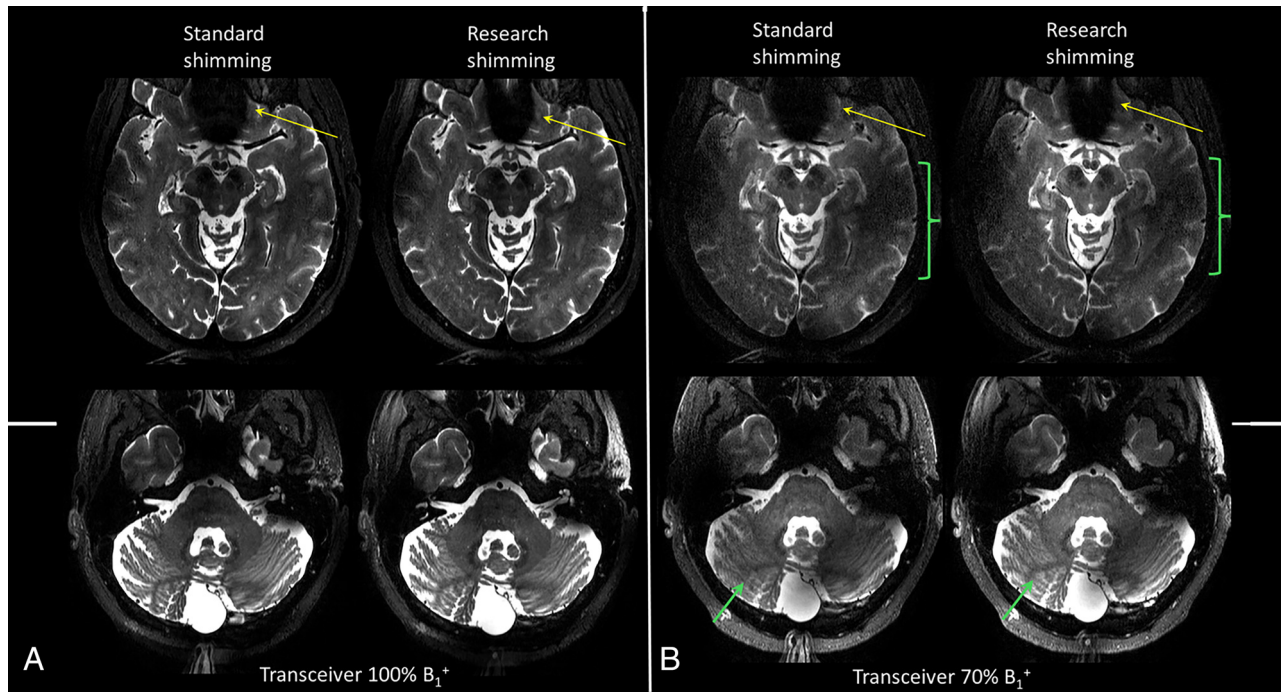


FIG 4. Matched subject T2 SPACE images acquired with the transceiver, showing the effect of insufficient B_1^+ and B_0 shimming. *A*, Images acquired with 100% B_1^+ , showing 2 axial planes at the midtemporal lobe and IAC-cerebellum. *B*, Matched images acquired with 70% B_1^+ showing the same 2 axial slices. With each axial slice, images acquired with standard and research shimming (comprising research shim optimization with VHOS hardware) are shown. All pairs are scaled identically between the transceiver and Nova 8/32. The *yellow arrows* highlight areas showing a B_0 effect; the *green identifiers* highlight areas showing a B_1^+ and B_0 interaction.

B_0 homogeneity is small; however in conditions with low B_1^+ , substantial B_0 inhomogeneity will cause signal shading and loss.

Limitations

The Z-longitudinal coverage of the transceiver was a limitation, as subjects with large heads did not fit well within the coil. This is demonstrated by our data (not all volunteers could be studied due to size). With this experience, we have implemented guidance (in addition to exclusions for claustrophobia) for body mass index restriction (<30 , not clinically obese) for the transceiver.

Another limitation was the lengthy acquisition durations due to SAR limitations applied when using RF shimming with the Terra. Improvements in acquisition time/coverage could be expected with more optimal SAR management and/or running with a fixed circularly polarized configuration. However, with the Nova 8/32, the B_1^+ differences between whole versus inferior brain would persist.

CONCLUSIONS

Overall, these methods give considerable improvement over standard strategies with more consistent imaging through the IAC, cerebellar hemispheres, and temporal lobes. The improvement is due to the transceiver's larger number of elements, their geometry, and decoupled design, providing better control over RF propagation, local SAR, and higher B_1^+ amplitudes inferiorly. Together with better B_0 homogeneity, these strategies allow limited bandwidth sequences such as the T2 SPACE sequence to more reliably image the IAC and inferior brain region. It is recognized however, for greater routine clinical utility, these methods

are limited based on subject head size. Expanding the cohort size, patient diversity and comparison with 3T at appropriate resolutions will be necessary to evaluate the broader applicability of the transceiver. Finally, it should be stated that with any coil strategy, deep learning methods may help to correct transmission and receptivity problems, although in this difficult location, demonstration with patient data will be needed.

Disclosure forms provided by the authors are available with the full text and PDF of this article at www.ajnr.org.

REFERENCES

- Bubrick EJ, Gholipour T, Hibert M, et al. 7T versus 3T MRI in the presurgical evaluation of patients with drug-resistant epilepsy. *J Neuroimaging* 2022;32:292–99 [CrossRef Medline](#)
- Verma G, Delman BN, Balchandani P. Ultrahigh field MR imaging in epilepsy. *Magn Reson Imaging Clin N Am* 2021;29:41–52 [CrossRef Medline](#)
- Bruschi N, Boffa G, Inglese M. Ultra-high-field 7-T MRI in multiple sclerosis and other demyelinating diseases: from pathology to clinical practice. *Eur Radiology Exp* 2020;4:59 [CrossRef Medline](#)
- Vaughan JT, Garwood M, Collins CM, et al. 7T vs. 4T: RF power, homogeneity, and signal-to-noise comparison in head images. *Magn Reson Med* 2001;46:24–30 [CrossRef Medline](#)
- Li S, Dardzinski BJ, Collins CM, et al. Three-dimensional mapping of the static magnetic field inside the human head. *Magn Reson Med* 1996;36:705–14 Nov [CrossRef Medline](#)
- Opheim G, van der Kolk A, Markenroth Bloch K, et al. 7T Epilepsy Task Force Consensus Recommendations on the Use of 7T MRI in Clinical Practice. *Neurology* 2021;96:327–41 [CrossRef Medline](#)
- Kim J, Sun C, Moon CH, et al. Evaluation of the performance of a 7-T 8×2 transceiver array. *NMR Biomed* 2024;37:e5146 [CrossRef Medline](#)

8. Pan JW, Lo KM, Hetherington HP. **Role of very high order and degree B0 shimming for spectroscopic imaging of the human brain at 7 Tesla.** *Magn Reson Med* 2012;68:1007–17 [CrossRef Medline](#)
9. Hetherington HP, Moon CH, Schwerter M, et al. **Dynamic B0 shimming for multiband imaging using high order spherical harmonic shims.** *Magn Reson Med* 2021;85:531–43 [CrossRef Medline](#)
10. Li X, Pan JW, Avdievich NI, et al. **Electromagnetic simulation of a 16-channel head transceiver at 7 T using circuit-spatial optimization.** *Magn Reson Med* 2021;85:3463–78 [CrossRef Medline](#)
11. van der Jagt MA, Brink WM, Versluis MJ, et al. **Visualization of human inner ear anatomy with high-resolution MR imaging at 7T: initial clinical assessment.** *AJNR Am J Neuroradiol* 2015;36:378–83 [CrossRef Medline](#)
12. Mugler JP, 3rd, Bao S, Mulkern RV, et al. **Optimized single-slab three-dimensional spin-echo MR imaging of the brain.** *Radiology* 2000;216:891–99 [CrossRef Medline](#)
13. Avdievich NI. **Transceiver-phased arrays for human brain studies at 7 T.** *Appl Magn Reson* 2011;41:483–506 [CrossRef Medline](#)
14. Gilbert KM, Curtis AT, Gati JS, et al. **A radiofrequency coil to facilitate B₁⁺ shimming and parallel imaging acceleration in three dimensions at 7 T.** *NMR Biomed* 2011;24:815–23 [CrossRef Medline](#)
15. Katscher U, Börnert P, Leussler C, et al. **Transmit SENSE.** *Magn Reson Med* 2003;49:144–50 [CrossRef Medline](#)
16. Grissom W, Yip C, Zhang Z, et al. **Spatial domain method for the design of RF pulses in multicoil parallel excitation.** *Magn Reson Med* 2006;56:620–29 [CrossRef Medline](#)